Optics Communications 445 (2019) 10–18

Contents lists available at ScienceDirect

Optics Communications

journal homepage: www.elsevier.com/locate/optcom

Theoretical analysis of long-haul systems adopting mode-division multiplexing

Abdulaziz E. Elfiqi [a,*], Abdallah A.I. Ali [b], Ziad A. El-Sahn [c], Kazutoshi Kato [d], Hossam M.H. Shalaby [c,e]

[a] Electronics and Electrical Communications Engineering Department, Faculty of Electronic Engineering, Menoufia University, Menouf 32952, Egypt
[b] Aston Institute of Photonic Technologies (AIPT), Aston University, Birmingham, B4 7ET, United Kingdom
[c] Photonics Group, Electrical Engineering Department, Alexandria University, Alexandria 21544, Egypt
[d] Graduate School of Information Science and Electrical Engineering, Kyushu University, Fukuoka 819-0395, Japan
[e] Electronics and Communications Engineering Department, Egypt-Japan University of Science and Technology (E-JUST), Alexandria 21934, Egypt

ARTICLE INFO

Keywords:
Few-mode fibers (FMF)
Gaussian noise model (GN-model)
Mode-division multiplexing (MDM)
Nonlinearity modeling
Space-division multiplexing (SDM)

ABSTRACT

In this paper, we modify the Gaussian noise model (GN-model) to address the nonlinearity effects in few-mode fibers. Closed-form expressions for the nonlinear interference power in birefringent few-mode fibers (FMFs) are derived and the effect of differential mode group delay (DMGD) is investigated. Moreover, the nonlinearity accumulation through propagation in multiple-spans fiber and the birefringence effect are considered. In addition, we discuss the effect of the DMGD on the fiber nonlinearity in systems adopting mode-division multiplexing (MDM). The results show that the DMGD management degrades the system performance in weak coupling regime because the nonlinear interference is enhanced. However, strong coupling-based transmission outperforms weak coupling transmission regardless of the DMGD effect in the weak coupling regime. On the other hand, by taking the DMGD effect into account, the system performance in weak coupling regime is better than that in strong coupling regime. Furthermore, the impact of the nonlinearity on the maximum reach is discussed.

1. Introduction

Optical transmission capacity is rapidly approaching its fundamental nonlinear limit in single mode fibers (SMFs) [1]. Optical space-division multiplexing (SDM) is a promising degree of freedom that increases the fiber transmission capacity. It supports multiple communication channels using modes in few-mode fibers (FMFs) and/or cores in multi-core fibers (MCFs) [2–4]. In recent years, several experimental efforts have been done to demonstrate optical space-division multiplexing based systems [5–7].

However, in long-haul transmission, the system performance suffers from physical impairments due to attenuation, dispersion, and nonlinearity. The fiber nonlinearity is a major source of capacity performance limitation [4,8–11]. This nonlinear limitation arises from the nonlinear interaction between different co-propagating optical fields due to Kerr-effects. These Kerr-effects simply involve nonlinear changes in the refractive index with increasing transmitted signal power, thus generating self-phase modulation (SPM), cross-phase modulation (XPM), or four wave mixing (FWM) [12–15]. Another linear interaction in FMFs transmission arises from the coupling between various spatial copropagating fields that results in a periodic-power transfer from an optical field to another copropagating one [11,16,17]. This linear coupling can exist: between dual-polarized fields on a specific mode (core), called linear polarization coupling, or (and) between different copropagating mode (core) fields, called linear mode coupling [17]. When the linear mode coupling level is comparable to that of polarization one, two distinct coupling regimes occur, namely weak- and strong-coupling regimes. In the weak coupling regime, the linear mode coupling is insignificant and could be neglected compared to the linear polarization coupling. On the other hand, in the strong coupling regime, the linear mode coupling is significant compared to the linear polarization coupling [16]. The randomly-varying birefringence during fiber transmission results in a reduction of the nonlinear interaction due to the randomly-averaging operation under the birefringence effect [16,18,19]. In the strong coupling regime, this randomly-averaging is higher compared to the weak coupling one, because of the large random-fluctuation of the propagating power in strong coupling case. Another linear propagation process in FMFs transmission is the differential mode group delay (DMGD) between the co-propagating modes [20,21]. It is similar to the differential group delay (DGD) between dual-polarized fields in SMFs transmission [22]. DMGD is a design limitation

* Corresponding author.
E-mail addresses: abdulaziz.elfiqi@ieee.org, abdulaziz.elfiqi@el-eng.menofia.edu.eg (A.E. Elfiqi), aliaai@aston.ac.uk (A.A.I. Ali), ziad.elsahn@ieee.org (Z.A. El-Sahn), kato@ed.kyushu-u.ac.jp (K. Kato), shalaby@ieee.org (H.M.H. Shalaby).

https://doi.org/10.1016/j.optcom.2019.04.003
Received 11 February 2019; Received in revised form 30 March 2019; Accepted 1 April 2019
Available online 4 April 2019
0030-4018/

of multiple-input–multiple-output (MIMO) receivers in MDM based systems [21,23]. Though the DMGD leads to an increase in the complexity of MIMO-receivers, it reduces the impact of nonlinearity of FMFs based transmission [24]. Further, a DMGD-management may be performed by periodically interchanging FMFs with different DMGDs in order to reduce the complexity of MIMO receivers [25].

Recently, the description of nonlinear propagation of dual-polarized signal through nonlinear-dispersive multi-mode optical fibers is described by the coupled multi-mode generalized nonlinear Schrödinger equation (MM-NLSE) and generalized coupled multi-mode Manakov equations [9,16,18,26,27]. The generalized multi-mode coupled Manakov equations are simpler than the MM-NLSE, but both have to be solved numerically by the split-step-Fourier-method (SSFM) [11,16]. Extensive efforts have been made for analytical modeling of the nonlinear interaction in SMFs using perturbative approaches [14,15,28–38]. In [14,15], an analytical model based on Volterra series transfer function (VSTF) has been developed to address the nonlinear impairments in long-haul transmission. One of these approaches is the well-known Gaussian noise model (GN-model), which is considered a reasonable-simple tool for addressing the nonlinearity [38]. The GN-model concept has been proposed in [36]. Then, it has been validated over a wide range of SMFs systems [37–41]. Recently, several extension efforts have been done on the GN model to enhance its accuracy and consider new features such as the impact of modulation formats and stimulated Raman scattering on long-haul transmission performance [42–46]. In this work, we discuss the nonlinear Kerr-effects for transmission over FMFs. For simplicity, we do not take into our consideration the impact of the modulation techniques and other nonlinear impairments. The GN-model is extended for FMFs transmission, since the nonlinear interference between two orthogonal-polarized fields is equivalent to that between two co-propagating spatial modes [47]. In recent years, some numerical and analytical efforts have been developed for evaluating this nonlinear propagation in FMFs [10,16,48–54]. In [50], an analytical analysis of the nonlinear interference in a weak coupled two-mode MDM based system has been introduced. In [4,10,51], the application of the GN-model in multi-mode fibers (MMFs) based systems has been validated. Furthermore, a generic expression for estimating the nonlinear information spectral density of MMFs based system has been proposed in [52]. In our previous work, we have just presented simple closed-form expressions for the nonlinear interference power for both weak- and strong coupling regimes [53,54].

The main contributions in this paper are summarized as follows.

- A complete mathematical analysis has been explored for obtaining closed-form expressions of the nonlinear interference power for both weak- and strong coupling regimes over FMFs based transmission systems.
- The effect of DMGD and its management in week coupling transmission is discussed.
- Expressions for the nonlinearity accumulation through multiple spans fiber propagation is presented.
- Analytical results illustrate the impact of nonlinearity on the bit-error rate (BER) performance under different system parameters, where the effect of both intra- and inter-modal nonlinearities are discussed.
- The impact of linear mode coupling is analytically explored.
- The impact of the nonlinearity on the maximum reach of different optical fiber schemes is discussed.

The remaining of this paper is organized as follows. In Section 2, we review the FWM in FMFs transmission and explore the derivation of simplified expressions for the phase-matching condition of FWM process for both weak- and strong-coupling regimes. The nonlinear propagation equations are also reviewed and the performance parameters are presented in same Section. In Section 3, a rigorous mathematical derivation for the modified GN-model in FMFs is detailed in order to obtain closed-form expressions for the nonlinear interference power in both coupling regimes. In addition, a scenario for the nonlinearity accumulation when propagating over multiple-spans fiber is discussed. In Section 4, our results of the derived expressions are discussed and compared to similar cases in literature. Finally, we give the conclusions in Section 5.

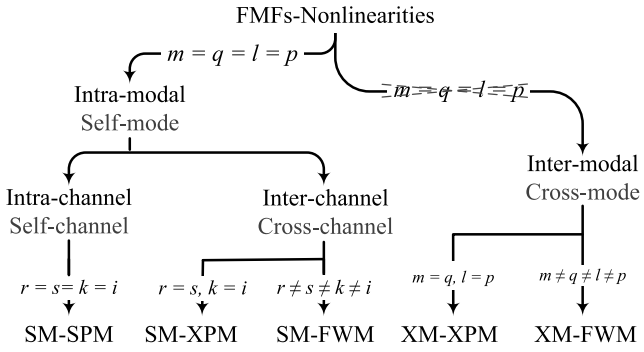

Fig. 1. Different nonlinear Kerr-effects in FMFs based system; SM-SPM: self-mode self-phase modulation, SM-XPM: self-mode cross-phase modulation, SM-FWM: self-mode four wave mixing, XM-XPM: cross-mode cross-phase modulation, XM-FWM: cross-mode four wave mixing. (r, s, k, i) and (m, q, l, p) are the frequencies and spatial modes indices, respectively.

2. General considerations

2.1. Four-wave-mixing in FMFs

The different nonlinear Kerr-effects that originate in FMFs transmission are summarized in Fig. 1. Self-phase modulation (SPM), cross-phase modulation (XPM), and four wave mixing (FWM) are third-order parametric processes that modulate the fiber refractive index [55,56]. These nonlinear effects can be classified into: (a) intra- and inter-channel nonlinearity based on the frequency channel interactions and (b) intra- and inter-modal nonlinearity based on space (mode) interactions [57,58]. Both SPM and XPM processes can be treated as special types of the FWM process [36]. For a FWM process in FMFs, the nonlinear interaction process among spatial fields at frequencies (f_r, f_s, f_k) results in an energy-transfer into an idler mode with a frequency (f_i), where (i, s, r, k) are the frequencies indices [59,60]. This FWM nonlinear-interaction occurrence among different spatial fields requires two conditions to be satisfied [51,55,59,60]: (1) a frequency (wavelength)/mode conservation condition $[if_0]_p = [rf_0]_m - [sf_0]_q + [kf_0]_l$, and (2) a phase-matching condition $\Delta\beta^{isrk}_{mqlp}(f_0) = \beta_m(rf_0) - \beta_q(sf_0) + \beta_l(kf_0) - \beta_p(if_0)$, where f_0 is the frequency separation between any two successive frequency-components and the subscripts (m, q, l, p) are the spatial modes indices.

Phase-matching condition

Simplified expressions for the phase-matching condition in FMFs can easily be formulated. For the weak coupling regime, the dispersion term of the pth mode can be expanded using Taylor's series as: $\beta_p(f) = \beta_{0_p} + 2\pi f\beta_{1_p} + 2\pi^2 f^2\beta_{2_p} + \cdots$, where β_{0_p}, β_{1_p}, and β_{2_p} are the propagation constant, the group delay (GD) parameter, and the group velocity dispersion (GVD) parameter, respectively. We focus our consideration to significant terms only (that is, up to the GVD term) [27,61]. By substituting this expansion in the phase-matching condition, we obtain

$$\begin{aligned}\Delta\beta^{isrk}_{mqlp}(f_0) =& (\beta_{0m} - \beta_{0q} + \beta_{0l} - \beta_{0_p}) + 2\pi[rf_o\beta_{1_m} - sf_0\beta_{1_q} \\ &+ kf_0\beta_{1_l} - if_0\beta_{1_p}] + 2\pi^2\{[rf_o]^2\beta_{2_m} - [sf_0]^2\beta_{2_q} \\ &+ [kf_0]^2\beta_{2_l} - [if_0]^2\beta_{2_p}\}. \end{aligned} \quad (1)$$

In birefringent-fiber transmission, both SPM and XPM effects are dominant compared to the FWM effect [16,47], thus the phase-matching

conditions for both XPM and SPM (i.e., $m = q$, and $l = p$) can be rewritten as:

$$\Delta\beta^{rski}_{ppqq}(f_0) = 2\pi\left[(r-s)\beta_{1_q} - (i-k)\beta_{1_p}\right] f_o + 2\pi^2\{[(rf_o)^2 - (sf_0)^2]\beta_{2_q} + [(if_0)^2 - (kf_0)^2]\beta_{2_p}\}. \quad (2)$$

Then, by applying the frequency conservation condition, i.e., $(rf_0 - sf_0 = if_0 - kf_0)$ and setting a simplified notation for $\Delta\beta^{isrk}_{ppqq}(f_0)$ as $\Delta\beta_{pq}(f_0)$, we get:

$$\Delta\beta_{pq}(f_0) = 2\pi\left\{(i-k)[\beta_{1_q} - \beta_{1_p}]f_o\right\} + 2\pi^2\{[(rf_o)^2 - (sf_0)^2]\beta_{2_q} + [(if_0)^2 - (kf_0)^2]\beta_{2_p}\}. \quad (3)$$

In order to obtain a continuous frequency-domain expression, we substitute: $if_0 \to f$, $kf_0 \to f_1$, $rf_0 \to f_2$, $sf_0 \to f_1 + f_2 - f$. This yields

$$\Delta\beta_{pq}(f) = 2\pi(f_1 - f)\Delta\beta_{1_{pq}} + 2\pi^2(f_1 - f)[(f_1 - f + 2f_2)\beta_{2_q} - (f_1 + f)\beta_{2_p}], \quad (4)$$

where $\Delta\beta_{1_{pq}} = \beta_{1_q} - \beta_{1_p}$ is the DMGD between spatial modes with indices p and q. At the center channel (i.e., $i = 0$), the last expression reduces to:

$$\Delta\beta_{pq} \approx 2\pi f_1(\Delta\beta_{1_{pq}} + 2\pi f_2\beta_{2_q}). \quad (5)$$

Moreover, for the intramodal case (i.e., $q = p$), the phase-matching condition is further simplified to: $\Delta\beta_{pp} \approx 4\pi^2 f_1 f_2 \beta_{2_p}$. Whereas, for strong coupling regime, the phase-matching condition is given by: $\Delta\beta \approx 4\pi^2 f_1 f_2 \hat{\beta}$, where $\hat{\beta}$ is the average GVD parameter of the co-propagating spatial modes for the strong coupling regime.

2.2. Signal propagation in FMFs

The frequency-domain electric-field propagating in FMFs can be expressed for the pth mode [16] as:

$$\bar{\mathbf{E}}_p(x, y, z, f) = F_p(x, y)\bar{\mathbf{A}}_p(z, f), \quad (6)$$

where $F_p(x, y)$ is the spatial field distribution and $\bar{\mathbf{A}}_p(z, f)$ is the slowly-varying field envelope vector for the pth mode as in [27]. According to [16], the nonlinear propagation in nonlinear-dispersive FMFs can be described by the generalized multi-mode coupled Manakov equation for the pth mode as follows

$$\frac{\partial\bar{\mathbf{A}}_p(z, f)}{\partial z} = \bar{\boldsymbol{\mathcal{L}}}_p(f)\bar{\mathbf{A}}_p(z, f) + \bar{\boldsymbol{\mathcal{G}}}_{nl_p}(z, f). \quad (7)$$

The right-hand side of (7) is divided into two terms: the first one is the linear part, where $\bar{\boldsymbol{\mathcal{L}}}_p(f)$ is a linear operator that includes both attenuation and dispersion operators, and the second term represents the source of nonlinear interference due to the Kerr-effects. Both $\bar{\boldsymbol{\mathcal{L}}}_p(f)$ and $\bar{\boldsymbol{\mathcal{G}}}_{nl_p}(z, f)$ are expressed based on the generalized multi-mode coupled Manakov equations for both coupling regimes in the following subsections 2.2.1 and 2.2.2. It is worth mentioning that there is another linear part due to the linear coupling between the co-propagating fields. However, the randomly-birefringence process averages out this linear part [16,19].

2.2.1. Weak coupling regime

In this regime, the linear operator is expressed as $\bar{\boldsymbol{\mathcal{L}}}_p(z, f) = -\bar{\boldsymbol{\alpha}}_p - \mathrm{j}\bar{\boldsymbol{\beta}}_p(f)$, where $\bar{\boldsymbol{\alpha}}_p$ and $\bar{\boldsymbol{\beta}}_p(f)$ are the fiber attenuation and dispersion operator for a dual-polarized field on the pth mode, respectively. Furthermore, the nonlinear term $\bar{\boldsymbol{\mathcal{G}}}_{nl_p}(z, f)$ is expressed as [16]

$$\bar{\boldsymbol{\mathcal{G}}}_{nl_p}(z, f) = \mathrm{j}\frac{4}{3}\gamma\sum_q^M f_{pq}\left(\frac{2}{3}\right)^{\delta_{pq}}\bar{\mathbf{A}}_q(z, f) * \left[\bar{\mathbf{A}}^{\star}_q(z, f)\right]^T * \bar{\mathbf{A}}_p(z, f). \quad (8)$$

Here, $\gamma = 2\pi n_2/(\lambda A_{\mathrm{eff}})$ is the fiber nonlinearity coefficient (with n_2 being the nonlinear-index coefficient, λ the propagating wavelength, and A_{eff} the core effective area of the fundamental mode), M is the number of the co-propagating modes, and δ_{pq} is the Kronecker delta function. The operator $*$ donates the convolution, and the superscripts T and $\star$ donate for the transpose and conjugation operators, respectively. The nonlinear interaction tensor $f_{pq} = f_{ppqq}$ between spatial modes with indices p and q is given by:

$$f_{ppqq} \overset{\mathrm{def}}{=} A_{\mathrm{eff}}\frac{\iint |F_p(x, y)|^2|F_q(x, y)|^2 dxdy}{\iint |F_p(x, y)|^2 dxdy \cdot \iint |F_q(x, y)|^2 dxdy}. \quad (9)$$

Note that the source of nonlinear interference part is classified into two distinct source-limited cases in FMFs; intramodal (self-mode modulation, SMM) and intermodal (cross-mode modulation, XMM) nonlinearity.

2.2.2. Strong coupling regime

In strong coupling regime, the linear operator is expressed as $\mathcal{L}_p(f) = -\hat{\alpha} - \mathrm{j}\hat{\beta}(f)$, where $\hat{\alpha}$ and $\hat{\beta}$ are the attenuation coefficient and average GVD parameter of the co-propagating spatial modes, respectively. The nonlinear term in (7) is expressed as [8,16]:

$$\bar{\boldsymbol{\mathcal{G}}}_{nl_p}(z, f) = \mathrm{j}\gamma\kappa\sum_q^M \bar{\mathbf{A}}_q(z, f) * \left[\bar{\mathbf{A}}^{\star}_q(z, f)\right]^T * \bar{\mathbf{A}}_p(z, f), \quad (10)$$

$$\text{where} \quad \kappa = \sum_{\substack{p,q\in\{1,2,\ldots,M\}:\\ q\le p}} \frac{32}{2^{\delta_{pq}}}\frac{f_{pq}}{6M(2M+1)}. \quad (11)$$

2.3. Performance parameters

To assess the performance of optical communication systems, it is essential to evaluate the bit-error rate (BER). It normally depends on the modulation format characteristics and is obtained in terms of the signal-to-noise ratio (SNR) based on the modulation techniques and its constellation cardinality [62–64]. Moreover, the SNR for the pth mode propagating in multiple-spans of FMFs can be expressed as [36]:

$$\mathrm{SNR}_p = \frac{B_n}{B_{ch}}\frac{P_{tx}}{P^{ac}_n + P^{ac}_{nl_p}}, \quad (12)$$

where B_n is the noise bandwidth, B_{ch} is the channel bandwidth, P_{tx} is the average lunch power per mode, and $P^{ac}_{nl_p}$ is the accumulated nonlinear interference power per mode, to be derived in Section 3. P^{ac}_n is the accumulated complex optical amplifier noise variance. For erbium-doped fiber amplifiers (EDFAs), it is simply the amplified-spontaneous-emission (ASE) noise per lumped amplifier, and is expressed as: $P_{\mathrm{ASE}} \approx (G-1)Fh\nu B_n$, where G is the amplifier gain, F is the amplifier noise figure, h is Plank's constant, and ν is the center-channel frequency [33,38,65].

3. Modified GN-model for mode-division multiplexing systems

In dual-polarized transmission over SMFs, the GN-model treats the nonlinearity as an independent additive Gaussian noise source, which is statistically independent from both the amplifier noise and the transmitted signal [38,61]. This can be applied to FMFs as the nonlinear interaction among the co-propagating spatial (mode) fields is equivalent to that among the orthogonal-polarized fields [47]. In the following subsections, we explore the modeling assumptions of the propagating signal, followed by detailed derivations of expressions for the nonlinear interference powers in both strong- and weak-coupling regimes.

3.1. Modeling assumptions

In order to apply a perturbation analysis such as the GN-model, some assumptions should be considered for the transmitted signal [38,51,52]: (1) the signal Gaussianity, (2) the statistical independence of the nonlinear interference from both the ASE noise and the transmitted signal, (3) the mode dependent loss is negligible, and (4) the relative low to moderate level of nonlinearity. A complex periodic process, which is spectrally shaped to satisfy the above assumptions, is used as a transmitted field envelope process at the input of the optical fiber ($z = 0$) using Karhunen–Loéve formula [62]:

$$A_{p_x}(0,f) = H_{p_x}(f)\sqrt{f_0}\sum_{\upsilon=-\infty}^{\infty}\vartheta_{\upsilon,p_x}\,\delta(f-\upsilon f_0), \tag{13}$$

where $H_{p_x}(f)$ is the transmitting filter shape, and ϑ_{υ,p_x} is a random variable of the pth mode on x-polarization at frequency (υf_0) having a zero mean $E\{\vartheta_{\upsilon,p_x}\} = 0$ and a unity variance $E\{|\vartheta_{\upsilon,p_x}|^2\} = 1$, such that E is the expectation operation.

We aim at obtaining an analytical model for the nonlinearity in FMFs, thus we should obtain a closed-form solution of (7) as:

$$\bar{\mathbf{A}}_p(z,f) = e^{\bar{\boldsymbol{\mathcal{L}}}_p z}\bar{\mathbf{A}}_p(0,f) + e^{\bar{\boldsymbol{\mathcal{L}}}_p z}\int_0^z e^{-\bar{\boldsymbol{\mathcal{L}}}_p z'}\bar{\boldsymbol{\mathcal{G}}}_{nl}(z',f)dz', \tag{14}$$

where $\bar{\mathbf{A}}_p(f)$ is the transmitted optical field envelope vector. A straightforward linear solution, $A_{l_{p_x}}(z,f)$, of (7) can be obtained by substituting (13) in the linear part of (14) as:

$$A_{l_{px}}(z,f) = H_{p_x}(f)\; e^{\boldsymbol{\mathcal{L}}_{p_x} z}\sqrt{f_0}\sum_{\upsilon=-\infty}^{\infty}\vartheta_{\upsilon,p_x}\delta(f-\upsilon f_0). \tag{15}$$

Obviously, obtaining the second part of the right hand side in (14) represents a big dilemma, because the source of nonlinear interference $\bar{\boldsymbol{\mathcal{G}}}_{nl}(z,f)$ is a function of both the linear and nonlinear solutions. Moreover, the nonlinear solution depends on the source of the nonlinear interference. Fortunately, the linear solution (15) can be used as a perturbative start for obtaining the nonlinear-solution part in (14) through the GN-model scenario, as will be shown in the following two subsections.

3.2. Nonlinear interference in weak coupling regime

In this subsection, we follow a similar procedure as in [33,37,51] to obtain an expression for the nonlinear interference power, $P^{w.}_{nl_p}$, in the weak coupling regime. We substitute the linear solution from (15) in the source of nonlinear interference $\bar{\boldsymbol{\mathcal{G}}}_{nl}(z,f)$ given by (8). We assume that all dual-polarized transmitting filter shapes are identical, i.e., $H_{p_x}(f_\upsilon) = H_{p_y}(f_\upsilon) = H_{q_y}(f_\upsilon) = H_{q_x}(f_\upsilon) = H(f_\upsilon)$. Then, we perform the triple convolution operation and apply the frequency condition: $(sf_0 - rf_0 + kf_0 = if_0)$. The expression of $\bar{\boldsymbol{\mathcal{G}}}_{nl}(z,f)$ for a particular mode at a specific frequency on x-polarization is obtained as:

$$\begin{aligned}\mathcal{G}^{w.}_{nl_{p_x}}(z,f_0) = \mathrm{j}\,\frac{4}{3}\,\gamma\, f_0^{\frac{3}{2}}\, e^{-3\alpha z}\sum_{q}^{M} f_{pq}\left(\frac{2}{3}\right)^{\delta_{pq}}\sum_{i=-\infty}^{\infty}\delta(f-if_0)\\ \times\sum_{r,s,k}\left[H(rf_0)H^{\star}(sf_0)H(kf_0)\right]\vartheta_{k,p_x}\left(\vartheta_{r,q_x}\vartheta^{\star}_{s,q_x}\right.\\ \left.+\;\vartheta_{r,q_y}\vartheta^{\star}_{s,q_y}\right)e^{-\mathrm{j}\left[\beta_q(rf_0)-\beta_q(sf_0)+\beta_p(kf_0)\right]z},\end{aligned} \tag{16}$$

where the superscript $w.$ denotes the weak coupling regime. We use (16) as a perturbative start to solve the dilemma of obtaining the second term of (14). By recalling the linear operator expression $\boldsymbol{\mathcal{L}}_p(f)$ and substituting by $[\beta_q(rf_0) - \beta_q(sf_0) + \beta_p(kf_0) - \beta_p(if_0) = \Delta\beta_{pq}(f_0)]$, we get the nonlinear optical field solution as:

$$\begin{aligned}A^{w.}_{nl_{p_x}}(z,f_0) = \mathrm{j}\frac{4}{3}\gamma f_0^{\frac{3}{2}} e^{-\alpha z}\sum_{q}^{M} f_{pq}\left(\frac{2}{3}\right)^{\delta^{pq}}\sum_{i=-\infty}^{\infty} e^{-\mathrm{j}\beta_p(if_0)}\delta(f-if_0)\\ \times\sum_{r,s,k}\left[H(rf_0)H^{\star}(sf_0)H(kf_0)\right]\left(\vartheta_{r,q_x}\vartheta^{\star}_{s,q_x}+\vartheta_{r,q_y}\vartheta^{\star}_{s,q_y}\right)\\ \times\vartheta_{k,p_x}\left[\frac{1-e^{-[2\alpha-\mathrm{j}\Delta\beta_{pq}(f_0)]z}}{2\alpha-\mathrm{j}\Delta\beta_{pq}(f_0)}\right].\end{aligned} \tag{17}$$

The power spectral density, $S^{w.}_{nl_{p_x}}(z,f_0)$, of the nonlinear interference can be obtained by statistically averaging the square absolute value of the nonlinear optical field $E\{A^{w.}_{nl_p}(z,f_0)A^{w.\star}_{nl_p}(z,f_0)\}$ as:

$$\begin{aligned}S^{w.}_{nl_{p_x}}(z,f_0) = \frac{16}{9}\gamma {f_0}^2 e^{-2\alpha z}\sum_{q}^{M} f_{pq}^2\left(\frac{4}{9}\right)^{\delta_{pq}}\sum_{i=-\infty}^{\infty}\delta(f-if_0)\\ \times\sum_{r,s,k}\left[H(rf_0)H^{\star}(sf_0)H(kf_0)\right]^2 E_{\vartheta\vartheta^{\star}}\eta^{r,s,k}_{\mathrm{FWM}}(f_0),\end{aligned} \tag{18}$$

where $\eta^{rsk}_{\mathrm{FWM}}(f_0) = |(1-e^{-[2\alpha-\mathrm{j}\Delta\beta_{pq}(f_0)]L_s})/(2\alpha-\mathrm{j}\Delta\beta_{pq}(f_0))|^2$ is the FWM efficiency [66], and $E_{\vartheta\vartheta^{\star}}$ is expressed as $E\{(\vartheta_{r,q_x}\vartheta^{\star}_{s,q_x}\vartheta_{k,p_x}+\vartheta_{r,q_y}\vartheta^{\star}_{s,q_y}\vartheta_{k,p_x})(\vartheta^{\star}_{r',q'_x}\vartheta_{s',q'_x}\vartheta^{\star}_{k',p'_x}+\vartheta^{\star}_{r',q'_y}\vartheta_{r',q'_y}\vartheta^{\star}_{k',p'_x})\}$.

The value of this expectation is altered for different nonlinearity limits. For intermodal nonlinearity limit (XMM), by recalling the random variable's properties at the state: $\{(q' = q, p = p')$ and $(r = r', s = s', k = k')\}$, the value of $E_{\vartheta\vartheta^{\star}}$ equals "2". For intramodal nonlinearity limit (SMM), the averaging operation is performed at the aforementioned state in the intermodal limit besides an additional new state: $\{(p = p')$ and $(s = k', r = r', k = s')\}$. This new state produces an additional "1" that makes the overall value of $E_{\vartheta\vartheta^{\star}}$ equals "3". So, the expression of the power spectral density (PSD) can be rewritten as follows

$$\begin{aligned}S^{w.}_{nl_{p_x}}(z,f_0) = \frac{32}{9}\gamma^2 f_0^3 e^{-2\alpha z}\sum_{q}^{M} f_{pq}^2\left(\frac{2}{3}\right)^{\delta_{pq}}\sum_{i=-\infty}^{\infty}\delta(f-if_0)\\ \times\sum_{r,s,k}\left[H(rf_0)H^{\star}(sf_0)H(kf_0)\right]^2\eta^{r,s,k}_{\mathrm{FWM}}(f_0).\end{aligned} \tag{19}$$

The same expression for y-polarization effect is obtained by performing similar analysis. The nonlinearity is evaluated at the span end where the amplifier compensates for the span loss. Thus, the overall PSD, i.e., $S^{w.}_{nl_p}(f_0) = S^{w.}_{nl_{p_x}}(f_0) + S^{w.}_{nl_{p_y}}(f_0)$ can be expressed by

$$\begin{aligned}S^{w.}_{nl_p}(f_0) = \frac{64}{9}\gamma^2 f_0^3\sum_{h} f_{pq}^2\left(\frac{2}{3}\right)^{\delta^{pq}}\sum_{i=-\infty}^{\infty}\delta(f-if_0)\\ \times\sum_{r,s,k}\left[H(rf_0)H^{\star}(sf_0)H(kf_0)\right]^2\eta^{r,s,k}_{\mathrm{FWM}}(f_0).\end{aligned} \tag{20}$$

The transmitting filter shape is assumed to be flat over the channel bandwidth, such that, $H_p(f_\upsilon) = (P_{tx}/2B_{ch})^{0.5}\,\mathrm{rect}(f_\upsilon)$ [61]. Furthermore, the discrete summation in (20) can be converted into continuous integral by setting $S^{w.}_{nl_p}(f) = \lim_{f_0\to 0} S^{w.}_{nl_p}(f_0)$. Thus, the PSD expression can be expressed as follows

$$S^{w.}_{nl_p}(f) = \frac{8\gamma^2}{9}\frac{P^3_{tx}}{B^3_{ch}}\sum_{q}^{M} f_{pq}^2\left(\frac{2}{3}\right)^{\delta_{pq}}\iint_D \eta_{\mathrm{FWM}}(f_1,f_2)df_1df_2. \tag{21}$$

Here D is the spectral integral area, shown as the dark-gray area in Fig. 2(a) and $\eta_{\mathrm{FWM}}(f_1,f_2) = \lim_{f_0\to 0}\eta^{r,s,k}_{\mathrm{FWM}}(f_0)$ is the FWM efficiency. $\eta_{\mathrm{FWM}}(f_1,f_2)$ can be expanded using the phase-matching condition in (5) and under the condition, $(\Delta\beta_{pq} \ll 2\alpha)$, at the center channel as:

$$\eta_{\mathrm{FWM}}(f_1,f_2) \approx \frac{L^2_{\mathrm{eff}}}{1+L^2_{\mathrm{eff,a}}\left[2\pi f_1(\Delta\beta_{1_{pq}}\delta_{pq}+2\pi f_2\beta_{2q})\right]^2}, \tag{22}$$

where $L_{\mathrm{eff}} = (1-e^{-2\alpha L_s})/2\alpha$ and $L_{\mathrm{eff,a}} = 1/2\alpha$ are the effective and asymptotic-effective lengths of a fiber with a span length L_s, respectively [38]. We use the approximation of the spectral bands into a square integration area, shown as light-gray area in Fig. 2(a). This spectral approximation is verified to give a closer result to the exact integral evaluation [67]. Furthermore, this approximation reduces the over-estimation of the nonlinear interference power in the GN-model. An analytical expression of the PSD, $S^{w.}_{nl_p}$, formulated by integrating the FWM efficiency in (22) over the light-gray area in Fig. 2(a) using the integration identities in [68]. Then, by integrating the obtained

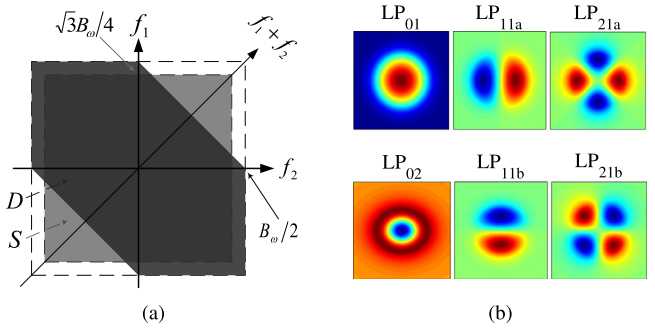

Fig. 2. (*a*) Spectral integration areas; D (dark-gray): the original integration area with limits $[-B_\omega/2,\ B_\omega/2]$ for all (f_1, f_2, f_1+f_2) and S (light-gray): the approximated square limits with a side length of $=\sqrt{3}B_\omega/2$, and B_ω is the total bandwidth, (*b*) Spatial field distribution for the six LP spatial modes.

analytical expression of the PSD over the noise bandwidth B_n, a closed-form expression for the per-span nonlinear interference power, $P^{w.}_{nl_p}$, can be obtained as:

$$P^{w.}_{nl_p} \approx \frac{4}{9\pi}\gamma^2 \frac{L^2_{\text{eff}}}{L_{\text{eff,a}}} \frac{B_n}{B^3_{ch}} P^3_{tx} \times \sum_q^M \frac{f^2_{pq}}{3^{\delta_{pq}}|\beta_{2_q}|} \left[arcsinh(\psi^+) + arcsinh(\psi^-)\right], \tag{23}$$

where $\psi^{\pm} = \frac{\sqrt{3}}{4}\pi L_{\text{eff,a}} B_\omega (\frac{\sqrt{3}}{2}\pi|\beta_{2_q}|B_\omega \pm \Delta\beta_{1_{pq}})$. Here $B_\omega = B_{ch}N_{ch}$ is the total WDM bandwidth, and N_{ch} is the number of the WDM channels.

3.3. Nonlinear interference in strong coupling regime

By starting from the MM-NLSE for strong coupling regime (10) and the phase-matching condition, we apply the same procedure as has been explored above in Section 3.2. The estimated value of $E_{\vartheta\vartheta\star}$ equals "3". A closed-form expression for the per-span nonlinear interference power, $P^{s.}_{nl_p}$, is thus obtained as:

$$P^{s.}_{nl_p} \approx \frac{3M}{8\pi} \frac{\gamma^2\kappa^2}{|\hat{\beta}_2|} \frac{L^2_{\text{eff}}}{L_{\text{eff,a}}} \frac{B_n}{B^3_{ch}} P^3_{tx} arcsinh\left(\frac{3}{8}\pi^2 L_{\text{eff,a}}|\hat{\beta}_2|B^2_\omega\right), \tag{24}$$

the superscript $s.$ denotes the strong coupling regime.

3.4. Accumulation of nonlinear interference over multiple spans

The accumulation scenarios of the nonlinear interference power through propagating over multiple-spans fiber can be viewed as either (*a*) coherent approach (accumulating nonlinear interference fields) [61], or (*b*) non-coherent approach (accumulating nonlinear interference powers). The second approach can be modified from a pure-linear variation with the number of spans N_s to a super-linear with an exponent ($\varepsilon < 1$), given by [69]:

$$\varepsilon \approx \begin{cases} \frac{3}{10}\ln\left(1 + \frac{12}{L_s}\frac{L_{\text{eff,a}}}{arcsinh(\psi^+)+arcsinh(\psi^-)}\right); & \text{weak,} \\ \frac{3}{10}\ln\left(1 + \frac{6}{L_s}\frac{L_{\text{eff,a}}}{arcsinh(\frac{3}{8}\pi|\hat{\beta}|L_{\text{eff,a}}B^2_\omega)}\right); & \text{strong.} \end{cases} \tag{25}$$

Thus, the total accumulated nonlinear interference power and total amplifier noise in (12) can be written as $P^{ac}_{nl_p} \approx N_s^{1+\epsilon} P_{nl_p}$ and $P^{ac}_n \approx N_s^{1+\epsilon} P_{\text{ASE}}$, respectively.

4. Results and discussions

In this section, we apply the modified GN-model to a generic long-haul hybrid wavelength-division multiplexing and mode-division multiplexing (WDM–MDM) system with the parameters similar to those in [16]. A step-index few-mode fiber (SI-FMF) is used as an optical channel for the weak coupling regime. This SI-FMF has a numerical aperture of 0.2, a core diameter of 12.5 μm, and a normalized frequency of $V \approx 5$ at a wavelength of 1.55 μm. It supports six linearly-polarized (LP) spatial modes (LP_{01}, LP_{11a}, LP_{02}, LP_{21a}, LP_{11b}, LP_{21b}). The spatial distributions of these LP modes are shown in Fig. 2(b) and their dispersion coefficient and DMGD are given in Table 1 [16, 70]. The fiber attenuation coefficient α of 0.22 dB/km and the nonlinear coefficient γ of 1.4 $W^{-1}km^{-1}$ are the same for all co-propagating modes. The calculated values of the nonlinear tensors ($f_{pq} = f_{ppqq}$) for the different LP modes are listed in Table 2. In addition, we study a graded-index few-mode fiber (GI-FMF) as the channel for the strong coupling regime. This GI-FMF supports different Hermitian Gaussian (HG) modes (HG_{00}, HG_{01}, HG_{02}+HG_{20}, HG_{11a}, HG_{10}, HG_{11b}) corresponding to the six LP modes of the SI-FMF [16]. The GI-FMF parameters are; fiber attenuation α, dispersion D, and nonlinear γ coefficients of 0.22 dB/km, 21.5 ps/km · nm, and 1.4 $W^{-1}km^{-1}$, respectively. We consider dual polarized-multiplexing quadrature phase-shift keying modulation with R_s = 28.5 GBaud, that equals to a net throughput of 25 GBaud and 14% of forward error correction (FEC) overhead. This corresponds to a WDM-channel bandwidth at the Nyquist border. EDFAs have 6 dB noise figure and a gain that compensates for the span loss, i.e., $G = e^{2\alpha L_s}$. The total fiber length is 1000 km with a span length of 100 km. These parameters are selected similar to those in [16] in order to be able to compare their trends.

Table 1
Dispersion coefficient; D [ps/km · nm], differential mode group delay; DMGD [ns/km], and core effective areas A_{eff} [μm^2] for the six LP spatial modes.

	LP_{01}	LP_{11a}	LP_{02}	LP_{21a}	LP_{11b}	LP_{21b}
D	25	27.3	−2.3	20.8	27.3	20.8
DMGD	0	6.5	9.9	12	6.5	12
A_{eff}	80	76	83	86	76	86

Table 2
Calculated values of f_{ppqq} for the six LP spatial modes.

	LP_{01}	LP_{02}	LP_{11a}, LP_{11b}	LP_{21a}, LP_{21b}
LP_{10}	1.000	0.734	0.661	0.455
LP_{02}	0.731	0.964	0.369	0.335
LP_{11a}, LP_{11b}	0.660	0.369	1.053	0.608
LP_{21a}, LP_{21b}	0.455	0.335	0.608	0.930

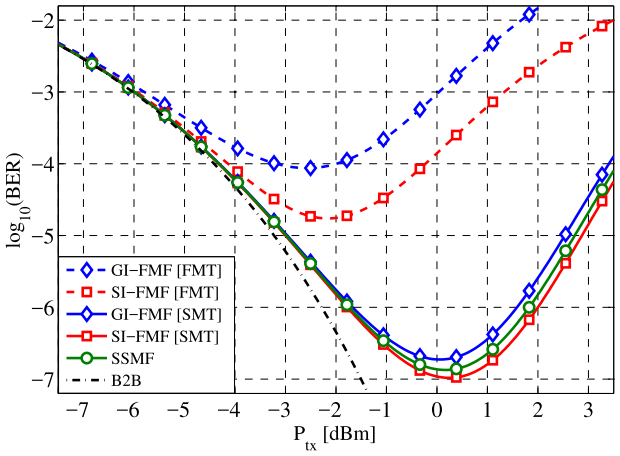

Fig. 3. Average BER versus average lunch power per mode for different transmission cases; B2B: back-to-back transmission (dashed–dotted), SSMF: standard single mode fiber (circles), SI-FMF: step-index few-mode fiber (squares), GI-FMF: graded-index few-mode fiber (diamonds), SMT: single-mode transmission (solid), FMT: full-mode transmission (dashed). The PM-QPSK/WDM–MDM system has $N_{ch} = 11$.

Fig. 3 illustrates the effect of the different nonlinear penalties on the performance of FMFs based systems. We opt the standard single-mode fiber (SSMF) as a reference case study with the parameters: $\alpha = 0.22\,\mathrm{dB/km}$, $D = 16.7\,\mathrm{ps/km\cdot nm}$, and $\gamma = 1.3\ \mathrm{W^{-1}\ km^{-1}}$ [61]. Here, we discuss two transmission cases for each coupling regime in FMFs. The first one is called single-mode transmission (SMT) corresponding to turning on the fundamental mode (LP_{01}) only. The second case is called full-mode transmission (FMT) corresponding to turning on all the six co-propagating modes. The bit-error rate (BER) averaged over all the turning-on modes is depicted as a function of the average lunch power per mode. In linear region, increasing the average lunch power enhances the system performance. However, after the average lunch power reaches a specific level (optimal average lunch power), the nonlinear interference power becomes significant compared to the noise power level. Beyond this power, any increase in the lunch power leads to a degradation of the system performance. This optimal average lunch power per mode, that achieves the minimum BER (minimal points on curves) [71], can be formulated in weak coupling regime as

$$P^{w.}_{tx_{\mathrm{opt}}} = \sqrt[3]{\frac{9\pi L_{\mathrm{eff,a}} B_{ch}^3 (G-1) F h\nu}{4\gamma^2 L_{\mathrm{eff}}^2 \sum_q^M \frac{f_{pq}^2}{3^{\delta_{pq}} |\beta_{2_q}|} [arcsinh(\psi^+) + arcsinh(\psi^-)]}}. \tag{26}$$

It is proportional to the WDM-channel bandwidth and inversely to both the nonlinear tensors values and the number of copropagating modes M. Moreover, the existence of the DMGD increases this optimal average lunch power value. It does not depend on the overall link length but on the fiber span length. Also, this power value is affected by the nonlinearity source-limited cases (SMM and XMM). Furthermore, in the strong coupling regime, the optimal average lunch power can be obtained as:

$$P^{s.}_{tx_{\mathrm{opt}}} = \sqrt[3]{\frac{8\pi |\hat{\beta}_2| L_{\mathrm{eff,a}} B_{ch}^3 (G-1) F h\nu}{3M\gamma^2\kappa^2 L_{\mathrm{eff}}^2\ arcsinh\left(\frac{3}{8}\pi^2 L_{\mathrm{eff,a}} |\hat{\beta}_2| B_\omega^2\right)}}. \tag{27}$$

For SMT case, the nonlinear interference results from the intramodal interaction. In GI-FMF based system (strong coupling regime), the intramodal nonlinear interference is higher than that in SSMF based system. Moreover, in SI-FMF based system (weak coupling regime), this intramodal nonlinear interference is lower than that for both GI-FMF and SSMF based systems. This performance is due to different propagation properties, i.e., the dispersion coefficient of the fundamental mode LP_{01} in SI-FMF based system is high compared to the other two fiber schemes. This leads to reducing the impact of nonlinearity in SI-FMF based system. In addition, the intramodal nonlinear penalty is altered with different fiber effective areas for various fiber schemes. On the other hand, for FMT case, the nonlinear interference results from both intra- and inter-modal nonlinear interactions. Thus, the difference in performance penalty between both FMT and SMT is due the intermodal nonlinear interference. For FMT case, it is noticed that the GI-FMF based system suffers more than the SI-FMF based system (taking the DMGD effect into account). This result is due to the impact of DMGD on the SI-FMF based system, which reduces the effect of nonlinearity compared to that of GI-FMF based system which is theoretically considered a fiber scheme with zero-DMGD. Although, the randomly-averaging of the nonlinear interference in the GI-FMF based system (strong coupling regime) is greater than that in the SI-FMF based system (weak coupling regime), the DMGD effect in SI-FMF based system is dominant over the effect of the randomly-averaging birefringence in the GI-FMF based system.

Fig. 4 depicts the impact of DMGD and its management on the performance of SI-FMF based system. The average BER is plotted versus the average lunch power per mode for different number of co-propagating (turning-on) modes in SI-FMF (weak coupling regime). Two propagation systems are investigated: unmanaged-DMGD SI-FMF (with DMGD values as given in Table 1) and managed-DMGD SI-FMF

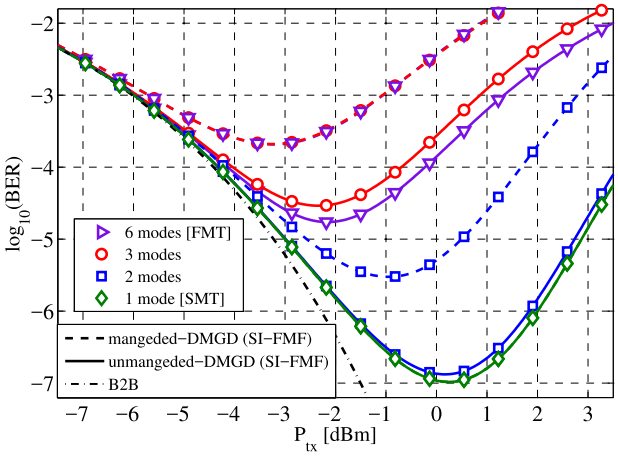

Fig. 4. Average BER versus average lunch power per mode in SI-FMF based system (weak coupling regime), for different transmission cases; one [SMT] (diamonds), two (squares), three (circles), and six [FMT] (triangles) modes, B2B: back-to-back transmission (dashed–dotted), for both unmanaged- (solid) and managed-DMGD (dashed) SI-FMF based system. The PM-QPSK/WDM–MDM system has $N_{ch} = 11$.

based systems. It is shown that, for SMT case, the performance of both unmanaged- and managed-DMGD propagating systems are identical. For three co-propagating modes (LP_{01}, LP_{11a}, LP_{02}) case, the optimal performance of unmanaged-DMGD system is degraded by about "1" order of magnitude when compared with the managed-DMGD one. This can be explained as follows. In the managed-DMGD system, the effect of the low dispersion coefficient of the third mode, LP_{02}, leads to high nonlinear interference. While, in the unmanaged-DMGD one, the effect of DMGD of LP_{02} compensates the effect of its low dispersion that reduces the overall nonlinear interference. For FMT case, the performance of unmanaged-DMGD system is better than that of three co-propagating modes. This performance can be explained as follows. By turning on the third mode (LP_{02}), its low dispersion coefficient results in higher nonlinear interference than that resulting form turning on one of the modes (LP_{11b}, LP_{21a}, LP_{21b}). Thus, the averaging over six modes results in an averaged BER value lower than that when turning on only three modes (LP_{01}, LP_{11a}, LP_{02}). On the other hand, the performance of managed-DMGD system is severely degraded when more than two modes are co-propagating, i.e., $M \in \{3, 4, 5, 6\}$. In addition, the average BER performance is approximately unchangeable. This performance is due to the low dispersion-coefficient of the mode (LP_{02}) when removing the DMGD effect. Specifically, for FMT case, the optimal performance of managed-DMGD system is degraded by about "1" order of magnitude compared with the unmanaged-DMGD system. In addition, the optimal power is reduced by about 1 dBm. Thus, the DMGD-management increases the overall nonlinearity effect compared to the DMGD-unmanaged based system. Fig. 4 shows a potential agreement with the conclusions in [24]. It is worth mentioning that DMGD-management is required to reduce the receiver complexity to achieve more realistic MDM receiver [24,25].

Fig. 5 illustrates the nonlinear penalty due to both intra- and inter-modal nonlinear interactions on the BER performance for various LP modes, in SI-FMF (weak coupling regime). The BER is drawn versus the OSNR (optical signal-to-noise ratio with respect to the ASE noise power with a reference noise bandwidth of 12.48 GHz (0.1 nm) [16]). Here, the single-mode transmission [SMT] is related to single transmission of any LP mode in a SI-FMF. For SMT case, the propagating spatial field suffers from only the intramodal nonlinearity. But, for FMT case, it suffers from both the intra- and inter-modal nonlinear interactions. Thus, the performance penalties between the two transmission cases is related to the intermodal nonlinear interaction. It is shown that all the modes (except LP_{02}) have almost the same intramodal nonlinearity penalty. The LP_{02} mode has a higher intramodal nonlinear interference because

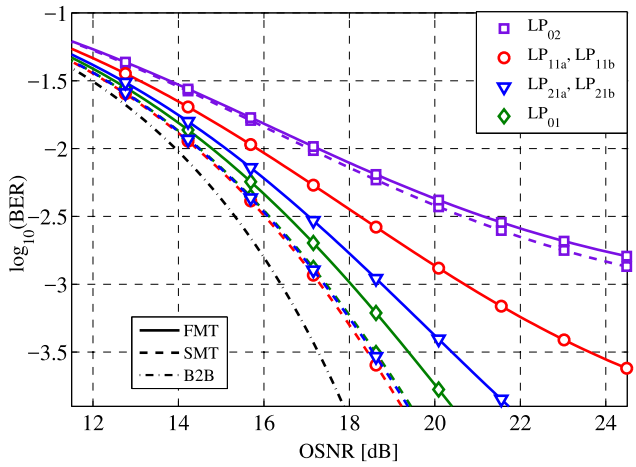

Fig. 5. BER versus OSNR for different LP modes in a SI-FMF based system, including SMT: single-mode transmission (dashed), FMT: full-mode transmission (solid), and B2B: back-to-back transmission (dashed–dotted). The PM-QPSK/MDM system has $N_{ch} = 1$ and $P_{tx} = 4$ dBm.

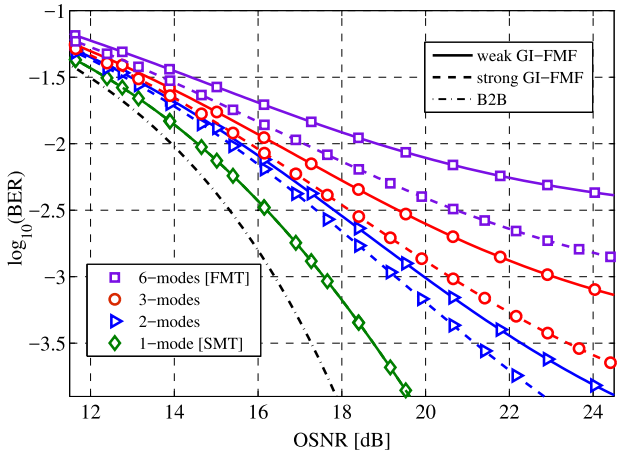

Fig. 6. Average BER versus OSNR for different number of co-propagating modes in GI-FMF, for weak- (solid), strong- (dashed) coupling regimes, and B2B: back-to-back transmission (dashed–dotted). The PM-QPSK/MDM system has $N_{ch} = 1$ and $P_{tx} = 4$ dBm.

of its low dispersion coefficient. Moreover, the non-degenerated modes (LP_{01} and LP_{02}) have lower intermodal nonlinear penalties compared with the degenerated ones (LP_{11v} and LP_{21v}). This is due to their degenerate nature that causes a high intermodal nonlinear penalty between $LP_{vv\mathrm{a}}$ and $LP_{vv\mathrm{b}}$ modes. In other words, these degenerated modes are affected by the same propagation characteristics. Specifically, at the FEC-requirement (BER $= 10^{-3}$), the FMT case suffers from an OSNR penalty of about 3 dB compared to the SMT case, for the $LP_{11a\ (b)}$ mode. This OSNR penalty is almost zero for the LP_{01} and LP_{02} modes.

Fig. 6 illustrates the impact of linear coupling on the system performance between different number of co-propagating modes in both coupling regimes, regardless of the effect of DMGD. The average BER is depicted versus OSNR for different number of co-propagating modes for both weak- and strong coupling in GI-FMF based system. Here we eliminate the DMGD effect in order to provide a fair comparison between the two distinct coupling regimes. Clearly, the performance of strong coupling regime is better than that of the weak coupling one in GI-FMF based system. The stronger linear mode coupling between the co-propagating modes, the higher variations in the propagating optical signal through the GI-FMF. This can be explained as follows. The nonlinear interference is reduced in the strong coupling GI-FMF compared to that in the weak coupling case. This nonlinearity reduction

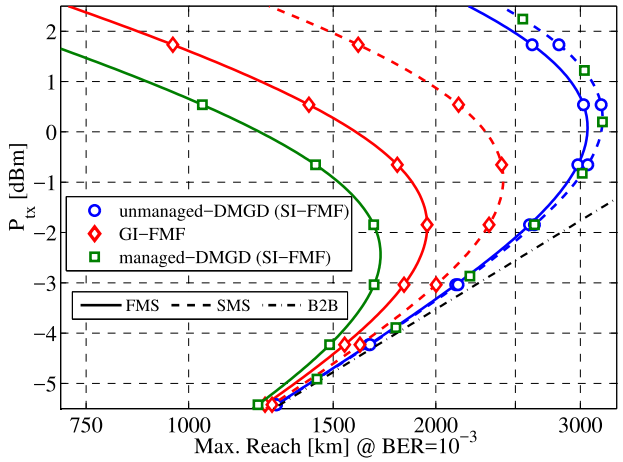

Fig. 7. Optical average lunch power versus fiber maximum reach for two distinct propagation systems: FMT (solid) and SMT (dashed) in different fibers; unmanaged-DMGD in SI-FMF (circles), managed-DMGD in SI-FMF (squares), and GI-FMF (diamonds). The PM-QPSK/WDM–MDM system has $N_{ch} = 11$.

in the strong coupling regime is due to the higher randomly-averaging birefringence operation compared to the weak coupling case that lacks the high linear coupling effect. Furthermore, it is shown that the more number of co-propagating modes, the higher degradation in performance of the weak coupling regime compared to that of strong coupling one. Turning on more co-propagating modes increases the total linear mode coupling on a specific mode. This leads to an increase in the nonlinearity compensation because of the high randomly-averaging birefringence operation of the nonlinear interference power in the strong coupling regime compared to the weak coupling one. The analytical results of Figs. 5 and 6 follow same trends in [16]. Thus, it gives a window of verification for the GN-model in MDM based systems by comparing our results with those in [16].

Fig. 7 shows the nonlinear penalty on the maximum distance that can be reached through various SI-FMF and GI-FMF for different co-propagation systems (SMT and FMT) at a BER of 10^{-3}. It is found that increasing the optical lunched power increases the achieved maximum reachable distance. But, after reaching a specific power the nonlinear interactions among co-propagating modes, this nonlinear interference power becomes significant compared to the amplifier noise, and then an optimal maximum reach is achieved. The aforementioned contributions of different fiber configurations are explored on the maximum reach. Specifically, the optimal maximum reach that could be achieved in the unmanaged-DMGD SI-FMF outreaches the GI-FMF case by about 777 km and 1100 km for both SMT and FMT, respectively. On the other hand, the managed-DMGD SI-FMF case reduces the optimal maximum reach by about 1350 km and 240 km compared to what can be achieved by the unmanaged-DMGD SI-FMF and GI-FMF systems, respectively.

5. Conclusions

The nonlinear interference penalty in birefringent few-mode fibers (FMFs) has been addressed by adapting the GN-model for weak- and strong-coupling transmission through FMFs based system. After a rigorous mathematical derivation, closed-form expressions for the nonlinear interference power have been derived. The nonlinearity accumulation and the DMGD effect through multiple-spans FMFs have been considered. The results show that the nonlinear penalty becomes significant beyond an optimal average lunch power that is inversely proportional to the number of co-propagating modes. The unmanaged-DMGD weak coupling transmission outperforms the strong coupling one due to the DMGD impact. On the other hand, regardless of the DMGD impact, the BER performance of strong coupling transmission is better than

that of the managed-DMGD weak coupling one. DMGD management increases the nonlinear penalty level and hence the optimal power is reduced, which results in a degradation of the corresponding optimal system performance in DMGD managed based systems. Furthermore, the birefringence effect in weak coupling-based system is lower than that in strong coupling based one. Thus, an increase in the level of the linear mode coupling (i.e., turning-on more modes) leads to a higher reduction in the nonlinearity of the weak coupling-based system compared to the strong coupling based one. The same effects of the nonlinearity on the maximum reach are noticed.

References

[1] R.-J. Essiambre, G. Kramer, P.J. Winzer, G.J. Foschini, B. Goebel, CaPacity limits of optical fiber networks, J. Lightwave Technol. 28 (4) (2010) 662–701.

[2] T. Mizuno, H. Takara, K. Shibahara, A. Sano, Y. Miyamoto, Dense space division multiplexed transmission over multicore and multimode fiber for long-haul transport systems, J. Lightwave Technol. 34 (6) (2016) 1484–1493.

[3] D.J. Richardson, J.M. Fini, L.E. Nelson, Space-division multiplexing in optical fibres, Nat. Photon. 7 (5) (2013) 354–362.

[4] G. Rademacher, R. Ryf, N.K. Fontaine, H. Chen, R. Essiambre, B.J. Puttnam, R.S. Luis, Y. Awaji, N. Wada, S. Gross, N. Riesen, M. Withford, Y. Sun, R. Lingle, Long-haul transmission over few-mode fibers with space-division multiplexing, J. Lightwave Technol. 36 (6) (2018) 1382–1388.

[5] P.J. Winzer, Making spatial multiplexing a reality, Nat. Photon. 8 (5) (2014) 345–348.

[6] R. Ryf, S. Randel, A.H. Gnauck, C. Bolle, A. Sierra, S. Mumtaz, M. Esmaeelpour, E.C. Burrows, R.-J. Essiambre, P.J. Winzer, et al., Mode-division multiplexing over 96 km of few-mode fiber using coherent 6 6 MIMO processing, J. Lightwave Technol. 30 (4) (2012) 521–531.

[7] J. Sakaguchi, B.J. Puttnam, W. Klaus, Y. Awaji, N. Wada, A. Kanno, T. Kawanishi, K. Imamura, H. Inaba, K. Mukasa, R. Sugizaki, T. Kobayashi, M. Watanabe, 19-core fiber transmission of 19x100x172-Gb/s SDM-WDM-PDM-QPSK signals at 305Tb/s, in: Optical Fiber Communication Conference, OFC, Los Angeles, CA, 2012, pp. 1–3.

[8] A. Mecozzi, C. Antonelli, M. Shtaif, Coupled Manakov equations in multimode fibers with strongly coupled groups of modes, Opt. Express 20 (21) (2012) 23436.

[9] C. Antonelli, M. Shtaif, A. Mecozzi, Modeling of nonlinear propagation in space-division multiplexed fiber-optic transmission, J. Lightwave Technol. 34 (1) (2016) 36–54.

[10] G. Rademacher, S. Warm, K. Petermann, Analytical description of cross-modal nonlinear interaction in mode multiplexed multimode fibers, IEEE Photonics Technol. Lett. 24 (21) (2012) 1929–1932.

[11] Nonlinear Performance of Few-Mode Fiber Links with Intermediate Coupling.

[12] J. Toulouse, Optical nonlinearities in fibers: review, recent examples, and systems applications, J. Lightwave Technol. 23 (11) (2005) 3625–3641.

[13] G.P. Agrawal, Nonlinear fiber optics: its history and recent progress [Invited], J. Opt. Soc. Amer. B 28 (12) (2011) A1.

[14] H. Song, M. Brandt-Pearce, Range of influence and impact of physical impairments in long-haul DWDM systems, J. Lightwave Technol. 31 (6) (2013) 846–854.

[15] H. Song, M. Brandt-Pearce, A 2-D discrete-time model of physical impairments in wavelength- division multiplexing systems, J. Lightwave Technol. 30 (5) (2012) 713–726.

[16] S. Mumtaz, R. Essiambre, G.P. Agrawal, Nonlinear propagation in multimode and multicore fibers: Generalization of the Manakov equations, J. Lightwave Technol. 31 (3) (2013) 398–406.

[17] G.P. Agrawal, S. Mumtaz, R.J. Essiambre, Nonlinear performance of SDM systems designed with multimode or multicore fibers, in: Optical Fiber Communication Conference and Exposition and the National Fiber Optic Engineers Conference, OFC/NFOEC, Anaheim, CA, 2013, pp. 1–3.

[18] D. Marcuse, C.R. Manyuk, P.K.A. Wai, Application of the Manakov-PMD equation to studies of signal propagation in optical fibers with randomly varying birefringence, J. Lightwave Technol. 15 (9) (1997) 1735–1746.

[19] C. Menyuk, Nonlinear pulse propagation in birefringent optical fibers, IEEE J. Quantum Electron. 23 (2) (1987) 174–176.

[20] K.-P. Ho, J.M. Kahn, Linear propagation effects in mode-division multiplexing systems, J. Lightwave Technol. 32 (4) (2014) 614–628.

[21] N. Bai, G. Li, Equalizer tap length requirement for mode group delay-compensated fiber link with weakly random mode coupling, Opt. Express 22 (4) (2014) 4247.

[22] M. Karlsson, Probability density functions of the differential group delay in optical fiber communication systems, J. Lightwave Technol. 19 (3) (2001) 324–331.

[23] Y. Weng, X. He, Z. Pan, Performance analysis of low-complexity adaptive frequency-domain equalization and MIMO signal processing for compensation of differential mode group delay in mode-division multiplexing communication systems using few-mode fibers, in: SPIE Optics and Optoelectronics, SPIE OPTO, San Francisco, CA, 2016, p. 97740B.

[24] G. Rademacher, S. Warm, K. Petermann, Nonlinear interaction in differential mode delay managed mode-division multiplexed transmission systems, Opt. Express 23 (1) (2015) 55.

[25] F. Ye, S. Warm, K. Petermann, Differential mode delay management in spliced multimode fiber transmission systems, in: Optical Fiber Communication Conference and Exposition and the National Fiber Optic Engineers Conference, OFC/NFOEC, Anaheim, CA, 2013, pp. 1–3.

[26] F. Poletti, P. Horak, Description of ultrashort pulse propagation in multimode optical fibers, J. Opt. Soc. Amer. B 25 (10) (2008) 1645–1654.

[27] G. Agrawal, Nonlinear Fiber Optics, fourth ed., Academic Press, Amsterdam; Boston, 2006.

[28] A. Mecozzi, C.B. Clausen, M. Shtaif, Analysis of intrachannel nonlinear effects in highly dispersed optical pulse transmission, IEEE Photonics Technol. Lett. 12 (4) (2000) 392–394.

[29] J. Tang, A comparison study of the Shannon channel capacity of various nonlinear optical fibers, J. Lightwave Technol. 24 (5) (2006) 2070–2075.

[30] A. Bononi, P. Serena, N. Rossi, E. Grellier, F. Vacondio, Modeling nonlinearity in coherent transmissions with dominant intrachannel-four-wave-mixing, Opt. Express 20 (7) (2012) 7777.

[31] K. Peddanarappagari, M. Brandt-Pearce, Volterra series transfer function of single-mode fibers, J. Lightwave Technol. 15 (12) (1997) 2232–2241.

[32] M. Nazarathy, J. Khurgin, R. Weidenfeld, Y. Meiman, P. Cho, R. Noe, I. Shpantzer, V. Karagodsky, Phased-array cancellation of nonlinear FWM in coherent OFDM dispersive multi-span links, Opt. Express 16 (20) (2008) 15777.

[33] W. Shieh, X. Chen, Information spectral efficiency and launch power density limits due to fiber nonlinearity for coherent optical OFDM systems, IEEE Photonics J. 3 (2) (2011) 158–173.

[34] A. Mecozzi, R.J. Essiambre, Nonlinear shannon limit in pseudolinear coherent systems, J. Lightwave Technol. 30 (12) (2012) 2011–2024.

[35] L. Beygi, E. Agrell, P. Johannisson, M. Karlsson, H. Wymeersch, A discrete-time model for uncompensated single-channel fiber-optical links, IEEE Trans. Commun. 60 (11) (2012) 3440–3450.

[36] H. Louchet, A. Hodzic, K. Petermann, Analytical model for the performance evaluation of DWDM transmission systems, IEEE Photonics Technol. Lett. 15 (9) (2003) 1219–1221.

[37] P. Poggiolini, G. Bosco, A. Carena, V. Curri, Y. Jiang, F. Forghieri, A detailed analytical derivation of the GN-model of non-linear interference in coherent optical transmission systems, 2012, arXiv:1209.0394 [physics].

[38] P. Poggiolini, The GN model of non-linear propagation in uncompensated coherent optical systems, J. Lightwave Technol. 30 (24) (2012) 3857–3879.

[39] A. Nespola, S. Straullu, A. Carena, G. Bosco, R. Cigliutti, V. Curri, P. Poggiolini, M. Hirano, Y. Yamamoto, T. Sasaki, J. Bauwelinck, K. Verheyen, F. Forghieri, GN-model validation over seven fiber types in uncompensated PM-16QAM nyquist-WDM links, IEEE Photonics Technol. Lett. 26 (2) (2014) 206–209.

[40] E. Torrengo, R. Cigliutti, G. Bosco, A. Carena, V. Curri, P. Poggiolini, A. Nespola, D. Zeolla, F. Forghieri, Experimental validation of an analytical model for nonlinear propagation in uncompensated optical links, Opt. Express 19 (26) (2011) B790.

[41] P. Johannisson, M. Karlsson, Perturbation analysis of nonlinear propagation in a strongly dispersive optical communication system, J. Lightwave Technol. 31 (8) (2013) 1273–1282.

[42] D. Uzunidis, C. Matrakidis, A. Stavdas, Closed-form FWM expressions accounting for the impact of modulation format, Opt. Commun. 440 (2019) 132–138.

[43] P. Poggiolini, A generalized GN-model closed-form formula, 2018, arXiv:1810.06545 [physics].

[44] P. Poggiolini, M.R. Zefreh, G. Bosco, F. Forghieri, S. Piciaccia, Accurate non-linearity fully-closed -form formula based on the GN/EGN model and large-data-set fitting, in: Optical Fiber Communication Conference (OFC), Optical Society of America, 2019, p. M1I.4.

[45] D. Semrau, R.I. Killey, P. Bayvel, A closed-form approximation of the Gaussian noise model in the presence of inter-channel stimulated Raman scattering, J. Lightwave Technol. (2019) 1–1.

[46] P. Poggiolini, Y. Jiang, Recent advances in the modeling of the impact of nonlinear fiber propagation effects on uncompensated coherent transmission systems, J. Lightwave Technol. 35 (3) (2017) 458–480.

[47] A. Mecozzi, C. Antonelli, M. Shtaif, Nonlinearities in space-division multiplexed transmission, in: Optical Fiber Communication Conference and Exposition and the National Fiber Optic Engineers Conference, OFC/NFOEC, Anaheim, CA, 2013, pp. 1–3.

[48] C. Koebele, M. Salsi, G. Charlet, S. Bigo, Nonlinear effects in mode-division-multiplexed transmission over few-mode optical fiber, IEEE Photonics Technol. Lett. 23 (18) (2011) 1316–1318.

[49] F. Ferreira, S. Jansen, P. Monteiro, H. Silva, Nonlinear semi-analytical model for simulation of few-mode fiber transmission, IEEE Photonics Technol. Lett. 24 (4) (2012) 240–242.

[50] X. Chen, A. Li, G. Gao, A.A. Amin, W. Shieh, Characterization of fiber nonlinearity and analysis of its impact on link Capacity limit of two -mode fibers, IEEE Photonics J. 4 (2) (2012) 455–460.

[51] G. Rademacher, K. Petermann, Nonlinear Gaussian noise model for multi-mode fibers with space-division multiplexing, J. Lightwave Technol. PP (99) (2016) 1–1.

[52] A.D. Ellis, N. Mac Suibhne, F.C.G. Gunning, S. Sygletos, Expressions for the nonlinear transmission performance of multi-mode optical fiber, Opt. Express 21 (19) (2013) 22834–22846.
[53] A.E. El-Fiqi, A. Ali, Z. El-Sahn, H. Shalaby, R. Pokharel, Evaluation of nonlinear interference in few-mode fiber using the Gaussian noise model, in: Conference on Lasers and Electro-Optics, CLEO2015, San Jose, CA, 2015, pp. JTH2A.53(1–2).
[54] A. Ali, A. El-Fiqi, Z. El-Sahn, H. Shalaby, R. Pokharel, Analytical formula of nonlinear interference in few-mode fibers in strong coupling regime, in: 17th International Conference on Transparent Optical Networks, ICTON, Budapest, Hungary, 2015, pp. We.D1.6(1–4).
[55] I. Kaminow, T. Li, A.E. Willner, Optical Fiber Telecommunications Volume VIB : Systems and Networks, sixth ed., Academic Press, Amsterdam ; Boston, 2013.
[56] G.P. Agrawal, Fiber-Optic Communication Systems, fourth ed., John Wiley & Sons, 2012.
[57] R.J. Essiambre, M.A. Mestre, R. Ryf, A.H. Gnauck, R.W. Tkach, A.R. Chraplyvy, Y. Sun, X. Jiang, R. Lingle, Experimental investigation of inter-modal four-wave mixing in few-mode fibers, IEEE Photonics Technol. Lett. 25 (6) (2013) 539–542.
[58] R.J. Essiambre, M.A. Mestre, R. Ryf, A.H. Gnauck, R.W. Tkach, A.R. Chraplyvy, Y. Sun, X. Jiang, R. Lingle, Experimental observation of inter-modal cross-phase modulation in few-mode fibers, IEEE Photonics Technol. Lett. 25 (6) (2013) 535–538.
[59] Y. Xiao, R.-J. Essiambre, M. Desgroseilliers, A.M. Tulino, R. Ryf, S. Mumtaz, G.P. Agrawal, Theory of intermodal four-wave mixing with random linear mode coupling in few-mode fibers, Opt. Express 22 (26) (2014) 32039–32059.
[60] A. Rogers, Polarization in Optical Fibers, Artech House, Norwood, MA, 2008, 00018.
[61] A. Carena, V. Curri, G. Bosco, P. Poggiolini, F. Forghieri, Modeling of the impact of nonlinear propagation effects in uncompensated optical coherent transmission links, J. Lightwave Technol. 30 (10) (2012) 1524–1539.
[62] J. Proakis, M. Salehi, Digital Communications, fifth ed., McGraw-Hill Science/Engineering/Math, Boston, 2007.
[63] F. Xiong, Digital Modulation Techniques, second ed., Artech House Telecommunications Library, Norwood, MA, USA, 2006.
[64] E. Grellier, A. Bononi, Quality parameter for coherent transmissions with Gaussian-distributed nonlinear noise, Opt. Express 19 (13) (2011) 12781.
[65] G. Bosco, P. Poggiolini, A. Carena, V. Curri, F. Forghieri, Analytical results on channel capacity in uncompensated optical links with coherent detection, Opt. Express 20 (17) (2012) 19610–19611.
[66] X. Chen, W. Shieh, Closed-form expressions for nonlinear transmission performance of densely spaced coherent optical OFDM systems, Opt. Express 18 (18) (2010) 19039–19054.
[67] S. Savory, Approximations for the nonlinear self-channel interference of channels with rectangular spectra, IEEE Photonics Technol. Lett. 25 (10) (2013) 961–964.
[68] A. Jeffrey, D. Zwillinger, Table of Integrals, Series, and Products, seventh ed., Academic Press, Amsterdam ; Boston, 2007.
[69] G. Bosco, R. Cigliutti, A. Nespola, A. Carena, V. Curri, F. Forghieri, Y. Yamamoto, T. Sasaki, Y. Jiang, P. Poggiolini, Experimental investigation of nonlinear interference accumulation in uncompensated links, IEEE Photonics Technol. Lett. 24 (14) (2012) 1230–1232.
[70] I. Gmez-Castellanos, R.M. Rodrguez-Dagnino, Intensity distributions and cutoff frequencies of linearly polarized modes for a step-index elliptical optical fiber, Opt. Eng. 46 (4) (2007) 045003–045003–11.
[71] A.E. El-Fiqi, A.E. Morra, S.F. Hegazy, H.M.H. Shalaby, K. Kato, S.S.A. Obayya, Performance evaluation of hybrid DPSK-MPPM techniques in long-haul optical transmission, Appl. Opt. 55 (21) (2016) 5614–5622.